Inorganic Chemistry

Article

pubs.acs.org/IC

Incorporation of Trinuclear Lanthanide(III) Hydroxo Bridged Clusters in Macrocyclic Frameworks

Michał J. Kobyłka, Katarzyna Ślepokura, Maria Acebrón Rodicio, Marta Paluch, and Jerzy Lisowski*

Department of Chemistry, University of Wrocław, 14 F. Joliot-Curie, 50-383 Wrocław, Poland

Supporting Information

ABSTRACT: A cluster of lanthanide(III) or yttrium(III) ions, $Ln_3(\mu_3\text{-}OH)_2$, (Ln(III) = Nd(III), Sm(III), Eu(III), Gd(III), Tb(III), Dy(III), Yb(III), or Y(III)) can be bound in the center of a chiral macrocyclic amines H_3L1^R, H_3L1^S, and H_3L2^S obtained in a reduction of a 3 + 3 condensation product of (1*R*,2*R*)- or (1*S*,2*S*)-1,2-diaminocyclohexane and 2,6-diformyl-4-methylphenol or 2,6-diformyl-4-*tert*butylphenol. X-ray crystal structures of the Nd(III), Sm(III), Gd(III), Dy(III), and Y(III) complexes reveal trinuclear complexes with Ln(III) ions bridged by the phenolate oxygen atoms of the macrocycle as well as by μ_3-hydroxo bridges. In the case of the Nd(III) ion, another complex form can be obtained, whose X-ray crystal structure reveals two trinuclear macrocyclic units additionally bridged by hydroxide anions, corresponding to a $[Ln_3(\mu_3\text{-}OH)]_2(\mu_2\text{-}OH)_2$ cluster encapsulated by two macrocycles. The formation of trinuclear complexes is confirmed additionally by ^{1}H NMR, electrospray ionization mass spectrometry (ESI MS), and elemental analyses. Titrations of free macrocycles with Sm(III) or Y(III) salts and KOH also indicate that a trinuclear complex is formed in solution. On the other hand, analogous titrations with La(III) salt indicate that this kind of complex is not formed even with the excess of La(III) salt. The magnetic data for the trinuclear Gd(III) indicate weak antiferromagnetic coupling ($J = -0.17$ cm^{-1}) between the Gd(III) ions. For the trinuclear Dy(III) and Tb(III) complexes the $\chi_M T$ vs T plots indicate a more complicated dependence, resulting from the combination of thermal depopulation of m_J sublevels, magnetic anisotropy, and possibly weak antiferromagnetic and ferromagnetic interactions.

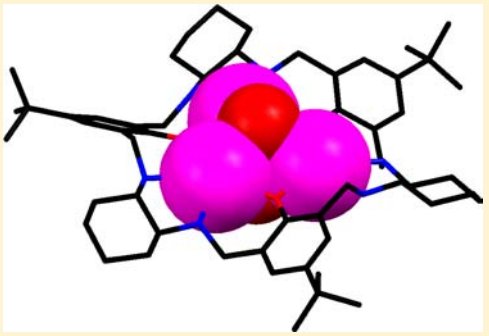

INTRODUCTION

Chiral 3 + 3 macrocycles (Figure 1) are interesting ligands that form a variety of lanthanide and transition metal complexes.[1−7] In a previous communication we have reported the X-ray crystal structure of a trinuclear, hydroxo-bridged Eu(III) complex of the deprotonated form of a large chiral macrocyclic amine $L1^R$ (Figure 1), and we have shown the encapsulation of the $Eu_3(\mu_3\text{-}OH)_2$ cluster within a macrocyclic environment.[1] In a more recent communication the synthesis of the analogous trinuclear Dy(III) complexes of L1 and analysis of their magnetic properties, consistent with single-molecule magnet (SMM) behavior, have been described.[2] Macrocycle $L1^R$ forms also mononuclear complexes with Ln(III) ions[3] as well as trinuclear complexes with transition metal ions.[4] Similarly, the related 3 + 3 macrocycle L3 forms mononuclear Ln(III) complexes[5] and trinuclear transition metal complexes,[6] while macrocycle L4, which is the 3 + 3 Schiff base analogue of L2, forms trinuclear double-decker zinc complexes[7] (Figure 1).

Here we describe the synthesis, spectroscopic characterization, magnetic properties, and crystal structures of a series of new trinuclear Ln(III) complexes of $L1^R$ and related macrocycles $L1^S$, $L2^R$, $L2^S$ (Figure 1). Since the applied macrocycles are chiral and can be obtained in an enantiopure form, their polynuclear complexes may combine magnetic properties with chirality.[8]

Lanthanide(III) ions exhibit interesting magnetic, spectroscopic, and chemical properties that are the basis of important applications of their complexes. The macrocyclic and chelate Gd(III) complexes are widely used in medical diagnostics as contrast enhancing agents for magnetic resonance imaging (MRI).[9] Ln(III) complexes are used also as catalysts, spectroscopic probes, and shift reagents and are tested as photosensitizers for cancer therapy and materials for liquid crystal displays. Some of the potential applications of Ln(III) compounds are related to polynuclear f-f complexes, and the coordination chemistry of these complexes attracts increasing attention. For instance complexes containing several Gd(III) ions are studied as improved contrast enhancing agents for MRI,[10] polynuclear complexes containing highly paramagnetic ions such as Gd(III), Dy(III), or Tb(III) are interesting molecular magnets,[11−14] and multimetallic lanthanide complexes are studied as artificial nucleases.[15,16] Despite many elegant molecular complexes containing more than one Ln(III) ion having been obtained,[17−19] the rational synthesis of molecular polynuclear lanthanide(III) complexes is still a challenging task. It is difficult to precisely control the coordination environment around the Ln(III) ion because of variable coordination numbers of Ln(III) ions, poorly defined steric and electronic requirements, and often highly fluxional character of their complexes.

One of the most important classes of polynuclear lanthanide(III) complexes is based on hydroxo-bridges. Many interesting

Received: February 27, 2013
Published: October 29, 2013

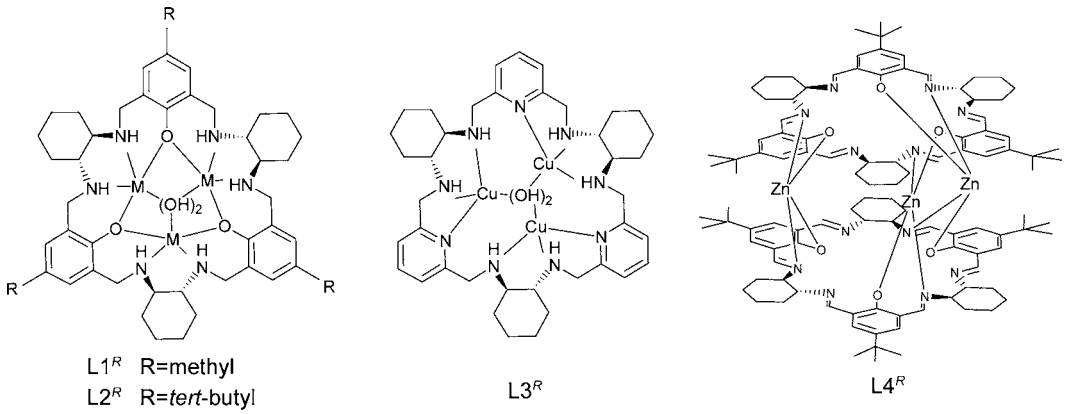

$[M_3LX_3(OH)_2]X$	M	L	X
1	Y	$L1^S$	Cl
2	Sm	$L1^R$	NO_3
3	Sm	$L1^S$	NO_3
4	Tb	$L1^R$	NO_3
5	Dy	$L1^R$	NO_3
6	Tm	$L1^R$	NO_3
7	Yb	$L1^R$	NO_3
8	Sm	$L2^S$	NO_3
9	Sm	$L2^R$	NO_3
10	Gd	$L2^S$	NO_3
11	Gd	$L2^R$	NO_3
12	Nd	$L2^S$	NO_3
13	Dy	$L2^S$	NO_3
14	Eu	$L2^S$	NO_3

Figure 1. Trinuclear complexes of macrocycles L1−L4 ((*RRRRRR*) isomers shown).

polynuclear hydroxo-bridged clusters[16,20] and coordination polymers[21] containing f-elements have been obtained, but their characterization was usually limited to the solid-state. On the other hand, the number of hydroxo-bridged polynuclear f-f complexes well-defined and well characterized in solution is much smaller.[18,19] Some of the polynuclear Ln(III) complexes contain the $Ln_3(\mu_3\text{-}OH)_2$ cluster, in particular the molecular complexes based on the $Dy_3(\mu_3\text{-}OH)_2$ core behave as single-molecule magnets (SMMs).[11] Similar trinuclear hydroxo-bridged structural motifs can be found in d-f magnetic materials,[14] in f-f coordination polymers,[21] and in Ln(III) clusters which are active in hydrolytic cleavage of DNA and RNA.[16]

EXPERIMENTAL SECTION

Syntheses. Macrocyclic amine $\mathbf{H_3L1^R}$ was synthesized as described previously,[22] the enantiomer $\mathbf{H_3L1^S}$ has been obtained similarly by reducing the corresponding 3 + 3 Schiff base derived from *trans*-(1*S*,2*S*)-diaminocyclohexane with $NaBH_4$.

$\mathbf{H_3L2^R}$, $\mathbf{H_3L2^S}$ were synthesized by reducing the analogous 3 + 3 Schiff base[7] with *tert*-butyl substituents. To the solution of (1*R*,2*R*)-1,2-diaminocyclohexane (1.00 g, 8.76 mmol) in 50 mL of acetonitrile, 2,6-diformyl-4-*tert*butylphenol (1.807 g, 8.76 mmol) was added. The resulting mixture became yellow, and the precipitate which was formed after 24 h of stirring at RT was collected and dried under vacuum. The formed Schiff base L4[7] (1.00 g, 1.17 mmol) was dissolved in 30 mL of methanol, and $NaBH_4$ (0.531 g, 14.04 mmol) was slowly added in for 1 h. The resulting mixture was evaporated to dryness, dissolved in water (200 mL), and then extracted with dichloromethane (2 × 100 mL). The collected organic fraction was dried over the potassium carbonate, filtered, and the solvent was removed giving a yellow solid. Yield: 88%. Anal. Calcd for $C_{54}H_{84}N_6O_3$: C, 74.96; H, 9.78; N, 9.71. Found: C, 75.05; H, 9.98; N, 9.59. ESI-MS - M(+) *m*/*z*: 865 $[H_4L2^R]^+$. ^1H NMR (500 MHz, CD_3OD): 1.05, 1.19, 1.28, 1.71, 2.18, 2.25, 3.74, 3.99, 7.03 ppm.

*$[Y_3L1^SCl_3(OH)_2]Cl{\cdot}4CH_3OH{\cdot}H_2O$ (**1**).* A solution of KOH (24.7 mg, 0.441 mmol) in 3 mL of methanol was added dropwise to the stirred solution of H_3L1^S (78.5 mg, 0.088 mmol) and $YCl_3{\cdot}6H_2O$ (133.8 mg, 0.441 mmol) in 10 mL of methanol. The resulting mixture was stirred for 40 h at RT and then left for slow evaporation of the solvent. After the total volume of the solution decreased by half, colorless crystals were formed. The crystal suitable for X-ray analysis was taken directly from the solution, and the rest of the sample was filtered and washed with small amount of cold methanol and dried in air. Yield: 26%. Anal. Calcd for $C_{49}H_{83}Cl_4N_6O_{10}Y_3$: C, 44.43; H, 6.32; Cl, 10.7; N, 6.34. Found: C, 44.54; H, 6.08; Cl, 10.35; N, 6.30. ^1H NMR (500 MHz, CD_3OD): 0.96 (m, 2H, $NHCHCH_2CH_2$-), 1.28 (m, 2H, $NHCHCH_2CH_2$-), 1.83 (m, 2H, $NHCHCH_2CH_2$−), 2.21 (s, 3H, $-CH_3$), 2.57 (m, 2H, $NHCHCH_2CH_2$-), 3.46 (m, 2H, $NHCHCH_2CH_2$−), 4.19 (br, 2H, $-CH_2$-), 6.98 (s, 4H, Ar*H*) ppm.

*$[Sm_3L1^R(NO_3)_3(OH)_2]NO_3{\cdot}8H_2O$ (**2**).* Solution of NaOH (13.4 mg, 0.335 mmol) in 2 mL of methanol was added dropwise to the stirred solution of H_3L2^R (82.5 mg, 0.112 mmol) and $Sm(NO_3)_3{\cdot}6H_2O$ (148.9 mg, 0.335 mmol) in 5 mL of methanol. The mixture was stirred for 20 h at room temperature (RT), and the obtained precipitate was filtered, washed with small amount of methanol, and dried under vacuum. Yield: 43.3%. Anal. Calcd for $C_{45}H_{81}N_{10}O_{25}Sm_3$: C, 33.50; H, 5.06; N, 8.68. Found: C, 33.38; H, 4.89; N, 8.63. ESI-MS - M(+) *m*/*z*: 1390 $[Sm_3L1^R(NO_3)_3(OH)_2]^+$, 663 $[Sm_3L1^R(NO_3)_2(OH)_2]^{2+}$. ^1H NMR (500 MHz, $CD_3OD/CDCl_3$, (v/v 1:1)): −6.58, 2.70, 2.75, 2.90, 3.50, 3.73, 4.44, 6.65, 13.32 ppm.

dx.doi.org/10.1021/ic400508y | *Inorg. Chem.* 2013, 52, 12893−12903

*$[Sm_3L1^S(NO_3)_3(OH)_2]NO_3{\cdot}10CH_3OH$ (**3**).* To the solution of H_3L1^S (6.1 mg, 0.0068 mmol) and $Sm(NO_3)_3{\cdot}6H_2O$ (9.1 mg, 20.6 mmol) dissolved in 1 mL of deuterated methanol in the NMR tube, a solution of KOH in deuterated methanol was added in portions. The final overall molar ratio of $L1^S$ to KOH was 1 to 5. After 48 h crystals suitable for X-ray analysis were formed in the NMR tube from which they were taken directly. The remaining crystals were filtered and washed with a small amount of cold methanol and dried in air. Yield: about 19%. Anal. Calcd for $C_{55}H_{105}N_{10}O_{27}Sm_3$: C, 36.91; H, 5.91; N, 7.83. Found: C, 37.10; H, 5.82; N, 7.90.

The compounds **4**–**7** were obtained according to the same procedure as the compound **2**. All of them were dried in vacuum.

*$[Tb_3L1^R(NO_3)_3(OH)_2]NO_3{\cdot}3.5H_2O$ (**4**).* Yield: 39.1%. Anal. Calcd for $C_{45}H_{72}N_{10}O_{20.5}Tb_3$: C, 34.68; H, 4.65; N, 8.99. Found: C, 34.74; H, 4.56; N, 8.90. ESI-MS - M(+) *m/z*: 1417 $[Tb_3L1^R(NO_3)_3(OH)_2]^+$, 677 $[Tb_3L1^R(NO_3)_2(OH)_2]^{2+}$. ^{1}H NMR (500 MHz, $CD_3OD/CDCl_3$, (v/v 1:1)): −29.2, −8.3, 10.0, 24.41, 39.2, 74.4, 100.0, 127.1, 183.0 ppm.

*$[Dy_3L1^R(NO_3)_3(OH)_2]NO_3{\cdot}6H_2O$ (**5**).* Yield: 30.8%. Anal. Calcd for $C_{45}H_{77}N_{10}O_{23}Dy_3$: C, 33.49; H, 4.81; N, 8.68. Found: 33.64; H, 4.86; N, 8.66. ESI-MS - M(+) *m/z*: 1427 $[Dy_3L1^R(NO_3)_3(OH)_2]^+$, 683 $[Dy_3L1^R(NO_3)_2(OH)_2]^{2+}$. ^{1}H NMR (500 MHz, $CD_3OD/CDCl_3$, (v/v 1:1)): 32.77, 62.23, 94.96, 102.00, 134.10, 179.80, 231.26 ppm.

*$[Tm_3L1^R(NO_3)(OH)_2]NO_3{\cdot}7H_2O$ (**6**).* Yield: 30.6%. Anal. Calcd for $C_{45}H_{79}N_{10}O_{24}Tm_3$: C, 32.74; H, 4.82; N, 8.43. Found: C, 32.53; H, 4.82; N, 8.27. ESI-MS - M(+) *m/z*: 1447 $[Tm_3L1^R(NO_3)_3(OH)_2]^+$, 693 $[Ho_3L1^R(NO_3)_2(OH)_2]^{2+}$. ^{1}H NMR (500 MHz, CD_3OD/D_2O, (v/v 1:1)): −262.0, −158.09, −97.0, −82.85, −65.67, −27.70, −23.70, 0.4, 19.0 ppm.

*$[Yb_3L1^R(NO_3)(OH)_2]NO_3{\cdot}11H_2O$ (**7**).* Yield: 28.6%. Anal. Calcd for $C_{45}H_{87}N_{10}O_{28}Yb_3$: C, 31.15; H, 5.05; N, 8.07. Found: 30.98; H, 4.50; N, 8.02. ESI-MS - M(+) *m/z*: 1458 $[Yb_3L1^R(NO_3)_3(OH)_2]^+$, 698 $[Yb_3L1^R(NO_3)_2(OH)_2]^{2+}$. ^{1}H NMR (500 MHz, CD_3OD/D_2O, (v/v 1:1)): −76.01, −48.05, −33.13, −25.00, −19.69, −13.88, −11.50, −9.77, 130.9 ppm.

*$[Sm_3L2^S(NO_3)_3(OH)_2]NO_3{\cdot}3CH_3OH{\cdot}3H_2O$ (**8**).* $Sm(NO_3)_3{\cdot}6H_2O$ (533.4 mg, 1.2 mmol) was added to the solution of $L2^S$ (346.1 mg, 0.4 mmol) dissolved in 10 mL of methanol and was stirred until it was completely dissolved. Triethylamine (0.28 mL, 2 mmol) was then added, and the solution was stirred again for 1 h and left at RT for the slow evaporation of the solvent without stirring. Four days later white crystals useful for X-ray analysis were formed. They were separated by decantation, washed with a small amount of methanol, and dried. Yield: 16.8%. Anal. Calcd for $C_{54}H_{95}N_{10}O_{23}Sm_3$: C, 38.08; H, 5.62; N, 8.22. Found: C, 37.93; H, 5.74; N, 8.37. ^{1}H NMR (500 MHz, CD_3OH/D_2O v/v 1/1): −6.43, 1.62, 2.60, 2.80, 3.22, 3.44, 3.57, 4.33, 4.66, 6.51, 7.97. ^{1}H NMR (500 MHz, CD_3OH): −4.13, −1.15, −0.52, 0.90, 1.46, 2.12, 2.29, 2.45, 2.78, 2.98, 3.51, 3.67, 3.87, 4.04, 4.36, 4.52, 4.65, 4.80, 5.46, 6.19, 6.33, 6.53, 6.58, 6.75, 6.85, 6.98, 7.69, 7.92, 8.27, 8.64, 9.26, 9.74, 10.90.

The compounds **9**–**14** were obtained according to the same procedure as the compound **8**.

*$[Sm_3L2^R(NO_3)_3(OH)_2]NO_3{\cdot}3CH_3OH{\cdot}3H_2O$ (**9**).* Yield: 23.6%. Anal. Calcd for $C_{57}H_{101}N_{10}O_{29}Sm_3$: C, 37.17; H, 5.54; N, 7.61. Found: C, 38.00; H, 5.80; N, 7.88. ^{1}H NMR is in accordance with the compound **8**.

*$[Gd_3L2^S(NO_3)_3(OH)_2]NO_3{\cdot}2CH_3OH{\cdot}2H_2O$ (**10**).* Yield 45.7%. Anal. Calcd for $C_{54}H_{95}Gd_3N_{10}O_{23}$: C, 37.23; H, 5.61; N, 8.04. Found: C, 37.24; H, 5.30; N, 7.80.

*$[Gd_3L2^R(NO_3)_3(OH)_2]NO_3{\cdot}2CH_3OH{\cdot}2H_2O$ (**11**).* Yield 45.7%. Anal. Calcd for $C_{54}H_{95}Gd_3N_{10}O_{23}$: C, 37.23; H, 5.61; N, 8.04. Found: C, 37.24; H, 5.30; N, 7.80. ESI-MS - M(+) *m/z*: 1458 714.7 $\{[Gd_3L_{-2H}](O)_2(NO_3)\}^{2+}$, 510.8 $[GdL_{-H}]^{2+}$.

*$[Nd_3L2^S(NO_3)_3(OH)_2]NO_3{\cdot}2CH_3OH{\cdot}2H_2O$ (**12**).* Yield 46.9%. Anal. Calcd for $C_{54}H_{95}Nd_3N_{10}O_{23}$: C, 38.44; H, 5.69; N, 8.30. Found: C, 38.24; H, 5.30; N, 8.10 . ^{1}H NMR (500 MHz, CD_3OH/D_2O v/v 1/1): −18.32, 0.81, 6.93, 7.32, 9.80, 10.59, 11.64, 12.23, 19.8171 (Figure 2).

*$[Dy_3L2^S(NO_3)_3(OH)_2]NO_3{\cdot}2CH_3OH{\cdot}2H_2O$ (**13**).* Yield 42.4%. Anal. Calcd for $C_{54}H_{95}Dy_3N_{10}O_{23}$: C, 37.27; H, 5.51; N, 8.05. Found: C, 37.94; H, 5.37; N, 8.15 .

*$[Eu_3L2^S(NO_3)_3(OH)_2]NO_3{\cdot}3CH_3OH{\cdot}3H_2O$ (**14**).* Yield 72.9%. Anal. Calcd for $C_{55}H_{101}Eu_3N_{10}O_{25}$: C, 37.57; H, 5.79; N, 7.97. Found: C, 37.37; H, 5.36; N, 7.83. ^{1}H NMR (500 MHz, CD_3OH/D_2O v/v 1/1): −22.31, −18.41, −12.05, −8.33, −6.85, −5.64, −4.39, −1.91, −0.61, 28.41 (Figure 2). ESI-MS - M(+) *m/z*: 1538.4 $[Eu_3L2^R(NO_3)_3(OH)_2]^+$, 738.2 $[Eu_3L2^R(NO_3)_2(OH)_2]^{2+}$.

*$[La_3(L1^S)_2(NO_3)_3]{\cdot}3CH_3OH{\cdot}H_2O$ (**15**).* A solution of KOH (35.0 mg, 0.625 mmol) in 5 mL of methanol was added dropwise to the stirred solution of H_3L1^S (112.0 mg, 0.125 mmol) and $La(NO_3)_3{\cdot}6H_2O$ (270.6 mg, 0.625 mmol) in 15 mL of methanol. The resulting mixture was stirred for 40 h at RT and then left for slow evaporation of the solvent. After the total volume of the solution decreased by half, colorless crystals were formed. The crystal suitable for X-ray analysis was taken directly from the solution, and the rest of the sample was filtered and washed with small amount of cold methanol and dried in air. Yield: 35%. Anal. Calcd for $C_{93}H_{140}N_{15}O_{19}La_3$: C, 51.03; H, 6.45; N, 9.60. Found: C, 51.10; H, 6.58; N, 9.55. ^{1}H NMR (500 MHz, CD_3OD): 0.26, 0.37, 0.56, 0.71, 0.99, 1.13, 1.50, 1.63, 1.75, 2.01, 2.10, 2.29, 2.41, 2.47, 2.70, 2.78, 2.81, 3.01, 3.09, 3.23, 3.42, 3.44, 3.47, 3.53, 3.56, 3.68, 3.81, 3.93, 4.70, 5.04, 6.43, 6.59, 6.77, 6.85, 6.98, 7.04 ppm. ESI-MS - M(+) *m/z*: 2111.7 $[La_3(L1^S)_2(NO_3)_3(H_2O)_2H]^+$.

Measurements. The NMR spectra were taken on Bruker Avance 500 and AMX 300 spectrometers. The positive-mode electrospray mass spectra of water/methanol solutions were obtained using a Bruker microOTOF-Q instrument. The elemental analyses were carried out on a Perkin-Elmer 2400 CHN elemental analyzer. The CD spectra were measured on a Jasco J-715 Spectropolarimeter. Electronic spectra were measured on a Cary 5 UV–vis-NIR spectrophotometer.

Variable temperature magnetizations (1.8–300 K) were measured using a Quantum Design SQUID-based MPMSXL-5-type magnetometer with field strength ranging from 0 to 5 T. The SQUID magnetometer was calibrated with the palladium rod sample. Background corrections for the sample holder and diamagnetic contribution estimated from the Pascal constants[23] were applied.

Crystal Structure Determination. The crystals of **1** and **8**–**13** were obtained by slow evaporation of the solvent from the mother liquor in which the syntheses were carried out. In case of compound **3** the crystals suitable for X-ray analysis were formed in the NMR tube from which they were taken directly.

The crystallographic measurements were performed at 90–120(2) K (Table 1) on a κ-geometry Xcalibur PX (ω and φ scan) or Kuma KM4CCD (ω scan) four-circle diffractometer with graphite-monochromatized MoK_α radiation. Data were corrected for Lorentz and polarization effects. Data collection, cell refinement, data reduction and analysis were carried out with Crysalis CCD and Crysalis RED, respectively.[24] Analytical or empirical (multiscan) absorption correction was applied to the data with the use of Crysalis RED. The structures of **1**, **3**, **8**, and **10** were solved by direct methods using the SHELXS-97 program[25] and refined on F^2 by a full-matrix least-squares technique using SHELXL-97[25] with anisotropic thermal parameters for the ordered and fully occupied non-H atoms. Some of the not fully occupied positions were also refined anisotropically. Because compounds **9**, **11**, **12**, and **13** are isomorphous with **10**, the refinements of their structures were started by using the coordinates of ordered heavy atoms taken from complex **10** (in the case of **9** and **11**, atom coordinates were changed into $-x+1$, $-y+1$, $-z+1$). All H atoms were treated as riding atoms in geometrically optimized positions, with O–H = 0.84–1.00 Å, N–H = 0.93 Å, C–H = 0.95–1.00 Å, and with U_{iso}(H) = 1.2U_{eq}(parent atom) for OH, NH, CH_2, or 1.5U_{eq}(parent atom) for Me–OH, CH_3. Water H atoms were not found in difference Fourier maps. Figures presenting the molecular structures were made with the DIAMOND[26] program.

All crystals are slightly disordered, mainly in the regions of axial ligands and uncoordinated solvent molecules or nitrate ions. **1** and **3** are mixed crystals containing two types of cations. In **1** two different complex cations may be distinguished in the same, symmetrically equivalent position: $[Y_3L1^SCl_3(OH)_2(MeOH)_2(H_2O)]^+$ with s.o.f. = 0.63(3) and $[Y_3L1^SCl_3(OH)_2(MeOH)(H_2O)_2]^+$ with s.o.f. = 0.37(3). Independently, the uncoordinated Cl^- ion is disordered into two positions with s.o.f. = 0.86(1), 0.14(1).

Similarly in **3**, two different complex cations may be distinguished in the same position: $[Sm_3L1^S(NO_3)_3(OH)_2(MeOH)_2(H_2O)]^+$ with

Table 1. Crystallographic Data of the Complexes 1, 3, and 8−13

	1	3	8	9	10	11	12	13
empirical formula	$C_{48.6}H_{82.2}Cl_4N_6O_{10}Y_3$	$C_{53.7}H_{101}N_{10}O_{26.3}Sm_3$	$C_{57}H_{101}N_{10}O_{23}Sm_3$	$C_{113.6}H_{198.8}N_{20}O_{44.8}Sm_6$	$C_{116}H_{206}Gd_6N_{20}O_{46}$	$C_{116}H_{206}Gd_6N_{20}O_{46}$	$C_{116}H_{206}N_{20}Nd_6O_{46}$	$C_{116}H_{206}Dy_6N_{20}O_{46}$
fw (g mol^{-1})	1319.13	1758.70	1745.53	3463.83	3560.51	3560.51	3482.45	3592.01
cryst syst	monoclinic	triclinic	trigonal	monoclinic	monoclinic	monoclinic	monoclinic	monoclinic
space group	$P2_1$ (No. 4)	$P\bar{1}$ (No.1)	$R3$ (No. 146)	$C2$ (No. 5)	$C2$ (No. 5)	$C2$ (No. 5)	$C2$ (No. 5)	$C2$ (No. 5)
a (Å)	14.036(7)	11.481(4)	20.874(3)	16.546(4)	16.783(4)	16.840(4)	16.754(4)	16.789(4)
b (Å)	14.916(5)	12.072(4)		20.898(4)	20.900(4)	20.925(4)	21.039(4)	20.843(4)
c (Å)	14.725(8)	12.900(4)	16.263(3)	22.017(4)	21.933(4)	21.945(4)	22.024(4)	21.923(4)
α (deg)		96.90(3)						
β (deg)	108.75(5)	91.94(3)		109.29(3)	109.39(3)	109.35(3)	109.66(3)	109.19(3)
γ (deg)		92.08(3)						
V (Å^3)	2919(2)	1772.5(10)	6136.8(17)	7186(3)	7257(3)	7296(3)	7311(3)	7245(3)
Z	2	1	3	2	2	2	2	2
T (K)	90(2)	100(2)	100(2)	100(2)	100(2)	120(2)	100(2)	100(2)
D_{calcd} (g cm^{-3})	1.501	1.648	1.417	1.601	1.629	1.621	1.582	1.646
μ (mm^{-1})	3.20	2.54	2.19	2.50	2.79	2.77	2.18	3.14
cryst size (mm)	0.27 × 0.23 × 0.12	0.21 × 0.15 × 0.02	0.20 × 0.12 × 0.09	0.36 × 0.27 × 0.22	0.17 × 0.10 × 0.09	0.32 × 0.26 × 0.14	0.17 × 0.16 × 0.05	0.19 × 0.15 × 0.07
radiation type	Mo Kα	Mo Kα	Mo Kα	Mo Kα	Mo Kα	Mo Kα	Mo Kα	Mo Kα
λ (Å)	0.71073	0.71073	0.71073	0.71073	0.71073	0.71073	0.71073	0.71073
θ range (deg)	4.77−26.00	4.71−26.00	3.23−35.00	4.69−29.00	2.86−29.99	4.76−26.00	2.86−30.00	2.85−30.00
index ranges	$-17 \le h \le 17$	$-13 \le h \le 14$	$-33 \le h \le 32$	$-20 \le h \le 22$	$-22 \le h \le 22$	$-20 \le h \le 20$	$-23 \le h \le 23$	$-22 \le h \le 23$
	$-14 \le k \le 18$	$-14 \le k \le 12$	$-33 \le k \le 33$	$-25 \le k \le 28$	$-29 \le k \le 27$	$-25 \le k \le 20$	$-28 \le k \le 29$	$-28 \le k \le 29$
	$-18 \le l \le 18$	$-15 \le l \le 15$	$-22 \le l \le 26$	$-30 \le l \le 30$	$-21 \le l \le 29$	$-27 \le l \le 27$	$-21 \le l \le 30$	$-26 \le l \le 30$
Tmin/Tmax	0.554/0.720	0.612/1.000	0.632/0.841	0.826/1.000	0.650/0.806	0.692/1.000	0.674/0.897	0.578/0.811
measured reflns	27900	14831	29958	40586	31314	46164	52885	47258
independent reflns	10609	11273	10473	16730	17583	13207	20710	20113
obsd reflns ($I > 2\sigma(I)$)	8850	9731	9147	14916	15002	12854	16784	17811
R_{int}	0.044	0.035	0.033	0.028	0.031	0.077	0.043	0.032
data/restraints/params	10609/25/661	11273/129/855	10473/38/265	16730/538/817	17583/310/847	13207/354/843	20710/367/845	20113/313/847
$R1$, $wR2$[a] ($F_o^2 > 2\sigma(F_o^2)$)	0.053, 0.128	0.049, 0.121	0.047, 0.124	0.042, 0.108	0.040, 0.089	0.044, 0.095	0.044, 0.100	0.033, 0.076
$R1$, $wR2$ (all data)	0.064, 0.130	0.060, 0.126	0.055, 0.127	0.050, 0.110	0.050, 0.091	0.045, 0.096	0.058, 0.104	0.041, 0.078
GOF = S	1.07	1.01	1.03	1.08	1.00	1.04	1.02	1.01
$\Delta\rho_{max}/\Delta\rho_{min}$ (e Å^{-3})	1.54/−1.13	2.76/−2.57	1.65/−0.84	1.28/−0.98	1.31/−0.78	1.78/−1.72	1.87/−1.63	1.36/−0.93
Flack parameter	0.02(1)	−0.02(2)	0.00(2)	0.02(2)	0.01(1)	0.04(2)	−0.01(1)	0.00(1)

[a] $R1 = \sum||F_o| - |F_c||/\sum|F_o|$; $wR2 = (\sum[w(F_o^2 - F_c^2)^2]/[w(F_o^2)^2])^{1/2}$. Detailed values of the weighting scheme (w) in each system are given in the crystallographic information file (CIF) provided as Supporting Information.

dx.doi.org/10.1021/ic400508y | Inorg. Chem. 2013, 52, 12893−12903

s.o.f. = 0.61(2) and $[Sm_3L1^S(NO_3)_3(OH)_2(MeOH)_3]^+$ with s.o.f. = 0.39(2). Additionally, the disorder of the complex cation is correlated with the disorder of the uncoordinated MeOH molecule (O4*M*−C4*M* with s.o.f. = 0.61(2)). Another uncoordinated MeOH molecule is not fully occupied (O10*M*−C10*M*, s.o.f. = 0.73(3)). Therefore, the formula $[Sm_3L1^S(NO_3)_3(OH)_2(MeOH)_2(H_2O)]_{0.6}[Sm_3L1^S(NO_3)_3(OH)_2(MeOH)_3]_{0.4}NO_3\cdot 6.3MeOH$, accepted in the final model, corresponds to the existence of two complexes, $[Sm_3L1^S(NO_3)_3(OH)_2(MeOH)_2(H_2O)](NO_3)\cdot 6.7MeOH$ and $[Sm_3L1^S(NO_3)_3(OH)_2(MeOH)_3](NO_3)\cdot 5.7MeOH$, randomly occupying the crystallographic sites of the unit cell in a 0.6:0.4 ratio.

The complex cation in $[Sm_3L2^S(NO_3)_3(OH)_2(H_2O)_3]NO_3\cdot 3MeOH$ (**8**) lies in a special position with the bridging OH groups lying on a 3-fold axis. The axial positions at the Sm(III) ion are occupied by nitrate ions and water molecules in a disordered manner. Thus, there are positions of three NO_3^- at the same face of the macrocyclic system, and corresponding positions of three water molecules at the opposite side, with s.o.f. = 0.60(2), and there are also reversed positions with s.o.f. = 0.40(2). This means that two different orientations of the same $[Sm_3L2^S(NO_3)_3(OH)_2(H_2O)_3]^+$ cation occur in the crystal lattice in a 0.6:0.4 ratio. The *t*-Bu groups of the macrocyclic ligand are disordered, and they were modeled with Me groups in two positions with s.o.f. = 0.59(2) and 0.41(2). Uncoordinated MeOH molecule is disordered into two sites with s.o.f. = 0.56(3) and 0.44(3). Uncoordinated nitrate counterions were not found in the refinement procedure. They are supposed to be highly disordered and fill the voids of about 320 Å^3 present in the crystal (960 Å^3 per unit cell volume of 6136.8(17) Å^3).

In the isomorphous crystals **9**, **10**, **11**, **12**, and **13**, of the general composition $\{[Ln_3L2^S(NO_3)_2(OH)_2(MeOH)_2(H_2O)_2](NO_3)_2\}\cdot[Ln_3L2^S(NO_3)_4(OH)_2(H_2O)_2]\cdot 6MeOH$ for **10**, **12**, and **13**, $\{[Ln_3L2^R(NO_3)_2(OH)_2(MeOH)_2(H_2O)_2](NO_3)_2\}\cdot[Ln_3L2^R(NO_3)_4(OH)_2(H_2O)_2]\cdot 6MeOH$ for **11**, and $\{[Sm_3L2^R(NO_3)_2(OH)_2(H_2O)_4]_{0.6}[Sm_3L2^R(NO_3)_2(OH)_2(MeOH)_2(H_2O)_2]_{0.4}(NO_3)_2\}\cdot[Sm_3L2^R(NO_3)_4(OH)_2(H_2O)_2]\cdot 4.8MeOH$ for **9**, both the complex cation (denoted as *A*) and the complex molecule (*B*) lie in a special position, that is on a 2-fold axis crossing Ln2, one of the aromatic rings (atoms O1, C1, C4, C5) and one of the cycohexyl ring (centers of two C−C bonds). All *t*-Bu groups are disordered and modeled with Me groups in two positions. The s.o.f. of these Me groups are equal to 0.5 for *t*-Bu groups lying on 2-fold axes, in other cases of *t*-Bu groups lying in general positions the s.o.f. values were refined; final s.o.f. = 0.56(2)/0.44(2) and 0.72(2)/0.28(2) for *A* and *B*, respectively in **12**, 0.56(2)/0.44(2) and 0.74(2)/0.26(2) for *A* and *B*, respectively in **9**, 0.60(2)/0.40(2) and 0.72(2)/0.28(2) for *A* and *B*, respectively in **10**, 0.59(2)/0.41(2) and 0.68(2)/0.32(2) for *A* and *B*, respectively in **11**, 0.64(2)/0.36(2) and 0.67(2)/0.33(2) for *A* and *B*, respectively in **13**. In complexes **9**, **10**, **11**, **12**, and **13**, one of the axial nitrate ions (denoted as N4) is disordered in both the complex cation (*A*) and complex molecule (*B*). This anion was modeled with some of the atoms disordered in two positions, that is, two O atoms of the NO_3^- group in two positions with s.o.f. = 0.69(2)/0.31(2) and 0.64(3)/0.36(3) for *A* and *B*, respectively in **12**, 0.64(2)/0.36(2) and 0.60(2)/0.40(2) for *A* and *B*, respectively in **10**, 0.62(2)/0.38(2) and 0.55(2)/0.45(2) for *A* and *B*, respectively in **13**, 0.65(3)/0.35(3) for *A* in **11**, N atom and two O atoms of the NO_3^- group in two positions with s.o.f. = 0.65(2)/0.35(2) for *A* in **9**, three O atoms of NO_3^- group in two positions with s.o.f. = 0.67(2)/0.33(2) for *B* in **9**, and all nitrate atoms in two positions with s.o.f. = 0.54(3)/0.46(3) for *B* in **11**. Additionally, for the complex cation *B* in **9** and **12**, the other nitrate ion is disordered and modeled with a N atom and two O atoms occupying two positions with s.o.f. = 0.51(2) and 0.49(2) (for **9**) or with three O atoms occupying two positions with s.o.f. = 0.57(2) and 0.43(2) (for **12**).

In addition to the disorder described above, **9** is a mixed crystal, because of the presence of two different complex cations (*A*) randomly occupying the crystallographic sites of the unit cell in a 0.6:0.4 ratio: $[Sm_3L2^R(NO_3)_2(OH)_2(H_2O)_4]^{2+}$ (with s.o.f. = 0.57(3)) and $[Sm_3L2^R(NO_3)_2(OH)_2(MeOH)_2(H_2O)_2]^{2+}$ (with s.o.f. = 0.43(3)). Because two out of three uncoordinated MeOH molecules are not fully occupied (s.o.f. = 0.67(2) for O3*M*−C3*M* and 0.66(2) for O4*M*−C4*M*), the finally accepted formula is $\{[Sm_3L2^R(NO_3)_2(OH)_2(H_2O)_4]_{0.6}[Sm_3L2^R(NO_3)_2(OH)_2(MeOH)_2(H_2O)_2]_{0.4}(NO_3)_2\}\cdot[Sm_3L2^R(NO_3)_4(OH)_2(H_2O)_2]\cdot 4.8MeOH$.

Some geometrical restraints (SADI, DFIX, SAME instructions in SHELXL-97), restraints on anisotropic displacement parameters (SIMU or ISOR instructions), as well as constraints on the fractional coordinates and anisotropic displacement parameters (EXYZ and EADP instructions) were applied in the refinement procedures if appropriate. Details are given in the crystallographic information file (CIF) provided as Supporting Information.

RESULTS AND DISCUSSION

Synthesis and Spectra. The macrocycles L1 and L2 react in methanol or water/methanol solvents with 3 equiv of lanthanide nitrates or chlorides and 5 equiv of base to give trinuclear complexes. Similar products are obtained with sodium hydroxide, potassium hydroxide, and triethylamine as a hydroxide source. These complexes can be obtained (with lower yields) also by using only 3 equiv of base. On the other hand, without the added base the reaction of these macrocycles with 3 equiv of lanthanide nitrates or chlorides results in mononuclear complexes of partially protonated macrocycles. The obtained trinuclear complexes dissolved in D_2O/CD_3OD give rise to simple ^{1}H NMR spectra consisting of 9 nonexchangeable lines, corresponding to effective D_3 symmetry (Figure 2).

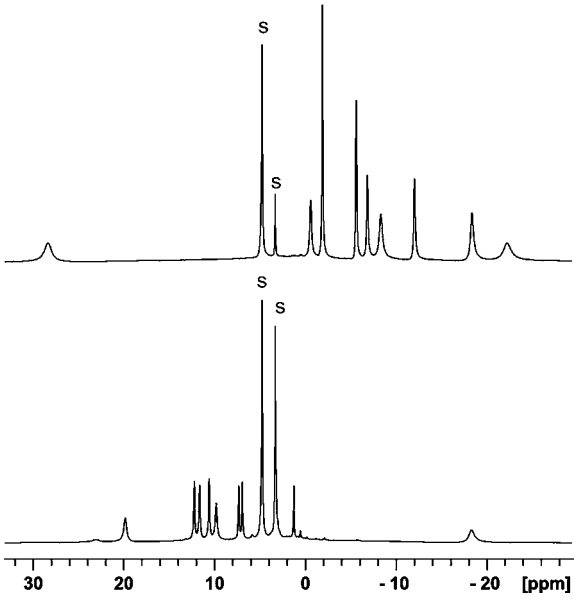

Figure 2. ^{1}H NMR spectra of **14** (top) and **12** (bottom) complexes (D_2O/CD_3OD, 298 K).

This spectral pattern easily distinguishes them from the mononuclear complexes of protonated macrocycles, $[LnH_4L(NO_3)_2](NO_3)_2$, which exhibit 26 nonexchangeable ^{1}H NMR signals corresponding to C_2 symmetry or the dinuclear complexes, such as $Na_3[Pr_2L(NO_3)_2(OH)_2]_2NO_3$, exhibiting 51 nonexchangeable ^{1}H NMR signals corresponding to C_1 symmetry.[3] The line widths of the discussed trinuclear Eu(III) and Nd(III) complexes are larger than those observed for other paramagnetic Nd(III) and Eu(III) macrocycles with similar metal-proton distances;[5,19] thus line broadening is probably a result of both paramagnetic relaxation and chemical exchange. The relatively broad bands indicate that the effective D_3 symmetry observed in solution likely results from the dynamic exchange of axial ligands (fast on the NMR time scale) among the various low-symmetry species. In particular this exchange seems to be more pronounced in

dx.doi.org/10.1021/ic400508y | Inorg. Chem. 2013, 52, 12893−12903

solutions containing water, where water molecule is probably the dominant axial ligand.

While the trinuclear Ln(III)complexes of L1 and L2 usually form easily in solution in the presence of excess of Ln(III) salts (except the largest Ln(III) ions) and base as judged by NMR spectra of species generated in situ, the isolation of pure solids in some cases was unsuccessful. For instance the reactions of the discussed macrocycles with samarium(III) nitrate or yttrium(III) chloride proceeded smoothly, but the analogous products obtained with yttrium(III) nitrate or lutetium(III) nitrate revealed complicated NMR spectra indicating mixtures of products.

We have also performed ^{1}H NMR titrations of the free ligand with 3 equiv of Y(III) (Figure 3, Supporting Information, Figure S1)) or Sm(III) (Supporting Information, Figure S2) salts and base. In both cases KOH was added in portions to the solution of H_3L1^S and Ln(III) salt until the final ratio of macrocycle to KOH reached 1: 5. These titrations indicate, that after the initial formation of mononuclear complex of protonated macrocycle and some other intermediate species finally a trinuclear complex is formed. After the completion of the titration in case of Sm(III) salt crystals of **3** were formed in the NMR tube. This constitute yet another evidence for the preference of the macrocycle to bind a $Ln_3(\mu_3\text{-}OH)_2$ cluster.

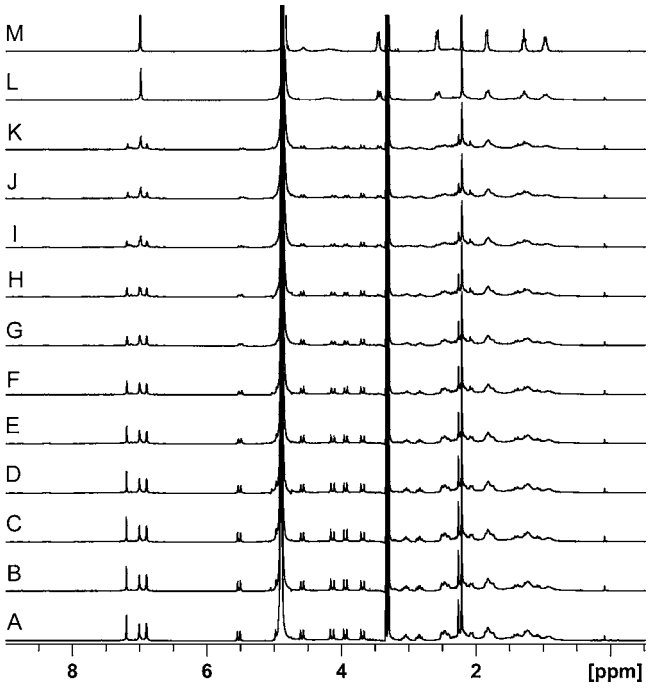

Figure 3. (A) ^{1}H NMR spectrum (CD_3OD) obtained after addition of 3 equiv of $YCl_3{\cdot}6H_2O$ to 1 equiv of H_3L1^S; (B–I) spectra obtained after subsequent additions of 0.5, 1.0, 1.5, 2.0, 2.5, 3.0, 4.0, and 5.0 equiv of KOH, respectively; (J–L) spectra of the sample I recorded after 24, 48, and 70 h, respectively; (M) the NMR spectrum of the crystals of the isolated complex **1**.

A different behavior was observed for the larger La(III) ion. In contrast to the heavier Ln(III) ions, the reaction of base and 3 (or even more) equiv of lanthanum(III) nitrate with $L1^S$ resulted in isolation of pure complex **15**, under conditions used for the synthesis of trinuclear derivatives. The ^{1}H and ^{13}C NMR spectra (Supporting Information, Figures S3 and S4) indicate C_1 symmetry of this complex. In particular the observation of six

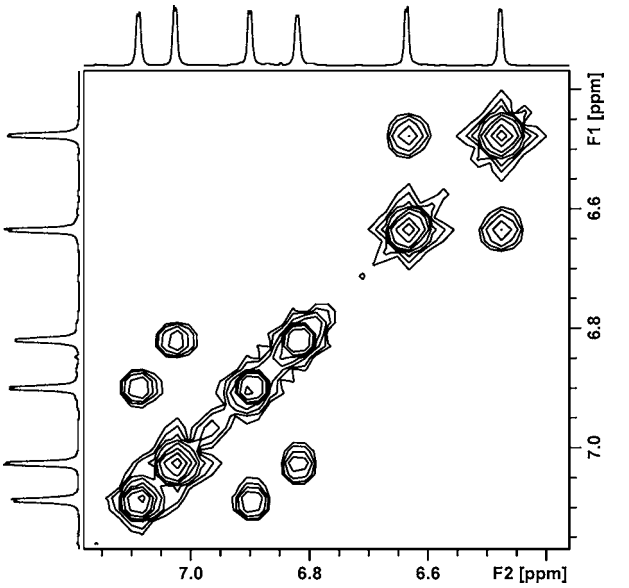

Figure 4. Aromatic region of the COSY spectrum of the lanthanum-(III) complex **15** ($CDCl_3$ solution).

signals of equal intensity in the aromatic region, corresponding to three pairs of correlated protons observed in the correlation spectroscopy (COSY) spectrum (Figure 4, Supporting Information, Figure S5) indicates the presence of three nonequivalent aromatic rings. Similarly total correlation spectroscopy (TOCSY) spectrum (Supporting Information, Figure S6) indicates three spin systems of cyclohexane proton signals in accord with C_1 symmetry observed previously in the crystal structure[3] of the dinuclear Pr(III) complex. The electrospray ionization mass spectrometry (ESI MS) spectra of **15**, exhibiting signals at *m/e* 2111.7 corresponding to cation $[La_3(L1^S)_2(NO_3)_3(H_2O)_2H]^+$, respectively, as well as elemental analyses indicate the presence of a complex containing two macrocyclic ligands and three lanthanum(III) ions. This formula is indeed supported by a preliminary X-ray crystal structure,[27] which indicates two dinuclear macrocyclic units with one La(III) ion shared over the two macrocycles. Thus, similarly as it was observed for Pr(III) derivative,[3] the macrocycle L seems to be unable to bind three larger La(III) ions and a dinuclear-type complex is formed instead.

To check whether the isolation of dinuclear-type La(III) complex was accidental, we have performed ^{1}H NMR titration of the free ligand H_3L1^S with La(III) salt and base under identical conditions which were applied for Y(III) and Sm(III) titrations. Indeed in the case of La(III) salts the initial formation of a mononuclear complex of a protonated macrocycle was followed by formation of complexes of lower symmetry, and the symmetric trinuclear species were not observed even with more than 3 equiv of La(III) used (Supporting Information, Figure S7). These experiment clearly shows that the size of the macrocycle L is too small to accommodate three larger Ln(III) ions.

The enantiopure character of the trinuclear complexes is reflected in their circular dichroism (CD) spectra. The intensive CD signals observed in the UV region correspond to organic chromophores on the ligand, as observed for the two isomers of the Gd(III) complexes **10** and **11** (Figure 5). For some complexes additional, much weaker signals corresponding to f-f transitions are also observed (Supporting Information, Figure S8)

dx.doi.org/10.1021/ic400508y | *Inorg. Chem.* 2013, 52, 12893–12903

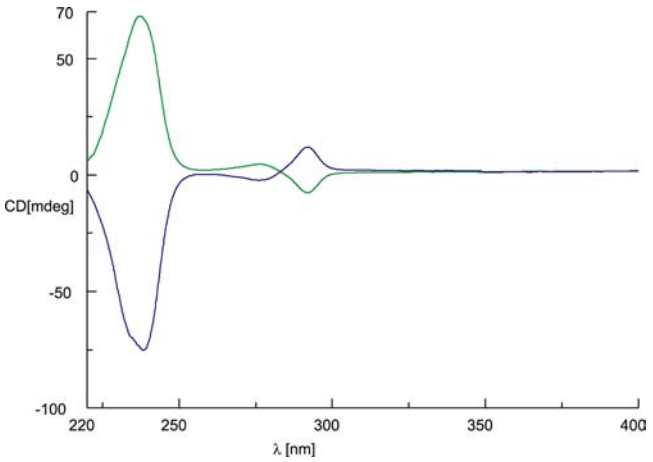

Figure 5. CD spectra of the enantiomeric trinuclear Gd(III) complexes **10** (blue) and **11** (green).

X-ray Crystal Structures. The X-ray crystal structures of the Nd(III), Sm(III), Gd(III), Dy(III), and Y(III) trinuclear complexes show incorporation of the $Ln_3(\mu_3\text{-}OH)_2$ cluster in the center of the macrocycles $L1^S$, $L2^R$, and $L2^S$. The three Ln(III) ions in these complexes are bridged by hydroxide anions and phenolate oxygen atoms to form an approximate equilateral triangle. In contrast to the situation observed for the mononuclear Ln(III) complexes,[3] the macrocycles adopt a relatively flat and symmetrical conformation. Several types of complex cations are observed in the solid state, which differ in the sets of axial ligands, nevertheless the lanthanide(III) ions are always eight-coordinate. The coordination spheres of Ln(III) ions in these trinuclear complexes correspond to irregular geometry and consist of two nitrogen atoms from the same cyclohexane ring, two bridging phenolate oxygen atoms, two bridging hydroxide anions, and two donor atoms from the axial anions or solvent molecules (one axial ligand is coordinated above and one below the macrocycle plane).

The asymmetric unit of complex **1** contains a cationic complex, two methanol molecules, and chloride anion disordered into two sites. The complex cation is of C_1 symmetry because of different set of axial ligands at each Y(III) ion; the first of these ions is coordinated by two methanol molecules, the second by chloride anion and water molecule, and the third Y(III) ion is coordinated by two chloride anions (Figure 6).

The compound **3** crystallizes in the *P*1 space group. The unit cell contains the cationic complex, ionic nitrate, and solvent molecules. The complex cation is again unsymmetrical; two Sm(III) ions are coordinated by a monodendate nitrate anion and methanol molecule, while the third Sm(III) ion is coordinated by a monodendate nitrate anion and water/methanol molecule (Figure 7).

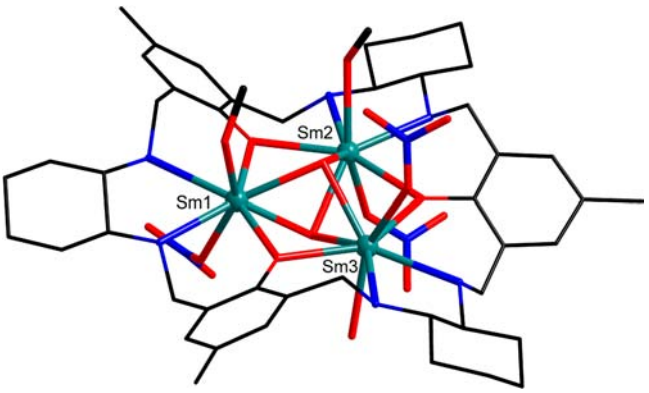

Figure 7. $[Sm_3L1^S(NO_3)_3(OH)_2(MeOH)_2(H_2O)]^+$, one of the complex cations present in **3**. H atoms are omitted for clarity.

The complexes **10**, **11**, **12**, and **13** crystallize in the *C*2 space group and are isomorphous. The contraction of lanthanide(III) ion radii in this series has a minimal influence on bond lengths (for selected bond lengths of **1**, **3**, **8**−**13** see Supporting Information, Table S1). Similarly the overall macrocycle radius, reflected, for example, by the distance between the outer cyclohexane carbon atom and the opposite *tert*-butyl group, is reduced only slightly by 0.2 Å when passing from the Nd(III) complex to the Dy(III) complex. Their crystals contain ionic nitrate, solvent molecules, as well as two different complex individuals: dication *A* and molecule *B* (Figure 8), both lying on a 2-fold axis as described earlier. The coordination environments of the individual Ln(III) ions incorporated in the complex cations *A* and molecules *B* are similar and differ only in axial ligands of one of the Ln(III) ions, that is, two lying in a general positions Ln1*A* and Ln1*B* are each coordinated by water molecule and monodentate nitrate anion, while located on a 2-fold axis Ln2 coordinates two MeOH molecules in *A* or two NO_3^- ions in *B*. In the structure of mixed crystal of compound **9**, another type of dication, namely $[Sm_3L2^R(NO_3)_2(OH)_2(H_2O)_4]^{2+}$ with two H_2O molecules at Sm2*A* is found beside $[Sm_3L2^R(NO_3)_2(OH)_2(MeOH)_2(H_2O)_2]^{2+}$ (see Figure 8 and Experimental Section).

The complex **8** crystallizes in the *R*3 space group. The complex cation of this crystal is of C_3 symmetry (lies on a 3-fold axis crossing both hydroxo bridges). Each Sm(III) ion is coordinated by an axial monodendate nitrate anion and an axial water molecule in disordered manner, as described in the Experimental Section. In each of the two orientations of the cation in the crystal, the NO_3^- ions are positioned at one side of

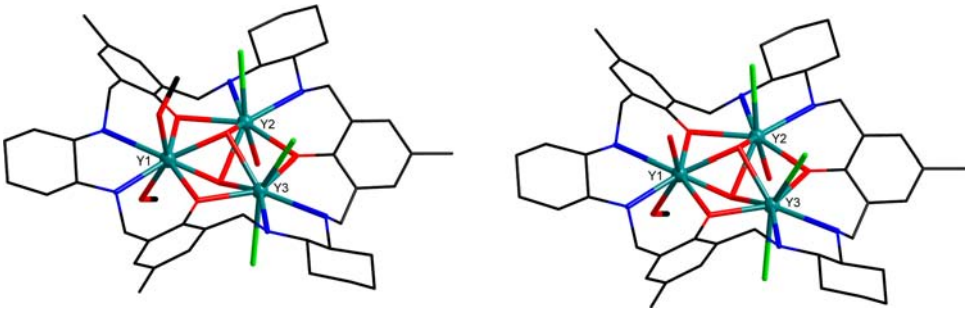

Figure 6. Two complex cations occupying the same position in **1**: $[Y_3L1^SCl_3(OH)_2(MeOH)_2(H_2O)]^+$ and $[Y_3L1^SCl_3(OH)_2(MeOH)(H_2O)_2]^+$. H atoms are omitted for clarity.

dx.doi.org/10.1021/ic400508y | *Inorg. Chem.* 2013, 52, 12893−12903

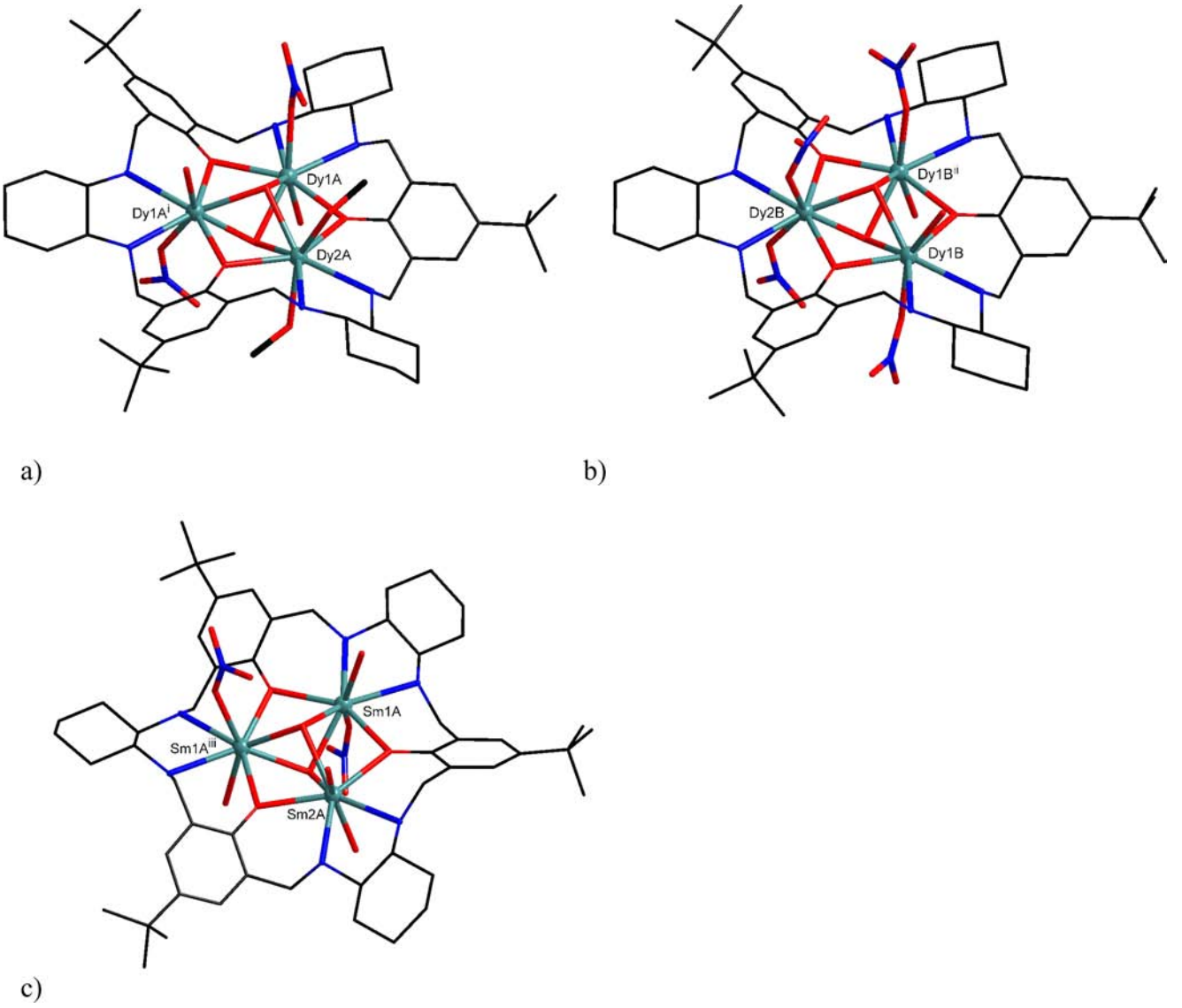

Figure 8. Views of the two independent complex forms in **13**, dication $[Dy_3L2^S(NO_3)_2(OH)_2(MeOH)_2(H_2O)_2]^{2+}$ (a) and molecule $[Dy_3L2^S(NO_3)_4(OH)_2(H_2O)_2]$ (b); the view of the $[Sm_3L2^R(NO_3)_2(OH)_2(H_2O)_4]^{2+}$ complex dication in **9** (c). H atoms and disorder of *t*-Bu groups and NO_3^- ions are omitted for clarity. Symmetry codes: (i) $-x+1, y, -z+1$; (ii) $-x, y, -z+1$; (iii) $-x+1, y, -z+2$.

the macrocycle (and the H_2O molecules at the other) (Figure 9, Supporting Information, Figure S9).

Out of 13 molecular structures of trinuclear complexes reported here, only the above trinuclear Sm(III) complex retains formally a 3-fold axis. Similarly, the trinuclear molecules observed in the previously reported structures of the $[Dy_3L1(\mu_3\text{-}OH)_2(NO_3)_2(H_2O)_4](NO_3)_2\cdot 6MeOH\cdot H_2O$ and $[Dy_3L1(\mu_3\text{-}OH)_2(SCN)_4(H_2O)_2]\cdot 3MeOH\cdot 2H_2O$ complexes[2] and $\{[Eu_3L1(NO_3)_2(OH)_2(H_2O)_3](\mu_2\text{-}NO_3)[Eu_3L1(NO_3)_3(OH)_2(H_2O)_2]\}(NO_3)_2\cdot 3.5CH_3OH\cdot 8H_2O$ complex[1] are devoid of a C_3 axis. The latter structure shows unsymmetrical trinuclear macrocylic units, additionally bridged by nitrate anion. This tendency to form low symmetry trinuclear complexes in the solid state seems to be an inherent feature of L1 and L2, and perhaps reflects less than perfect matching between the size of metal ions and the size of central core of the macrocycle. On the other hand the apparent C_3 symmetry resulting from fast exchange of axial ligands is observed in solution, as discussed above.

Although the complexes **8** and **9** give identical NMR spectra and mirror CD spectra they crystallize in different crystal forms. This effect reflects the delicate balance between different crystalline forms which are determined by slightly different crystallization conditions. The precise form of the obtained crystal is dependent more on crystallization time, solvents, and concentrations, rather than the variations of metal ion radius in the group of Nd(III), Sm(III), Eu(III), Gd(III), Dy(III), and Y(III) ions. In particular, partial hydrolysis of lanthanide(III) ions during crystallization may lead to the generation of additional hydroxide anions. Further dependence of the kind of the obtained form of the complex on the crystallization conditions is illustrated by the attempted synthesis of dinuclear Nd(III) complex based on the application of 2 equiv of neodymium nitrate per macrocycle. In this case the pure complexes were not obtained, but the single crystals of trinuclear complex were manually separated. Although their X-ray crystal structure could not be satisfactory solved, in this case the structural model (Figure 10, Supporting Information, Figure 10) shows yet another type of trinuclear complex of L2. Unlike the case of the above-discussed trinuclear complexes, only a single central μ_3-OH bridge connects the three Nd(III) ions bound by the

dx.doi.org/10.1021/ic400508y | *Inorg. Chem.* 2013, 52, 12893−12903

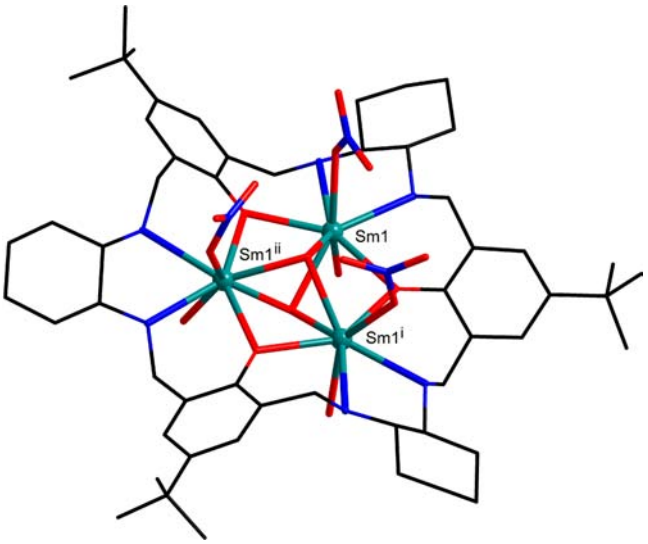

Figure 9. $[Sm_3L2^S(NO_3)_3(OH)_2(H_2O)_3]^+$ in **8**. H atoms and disorder of *t*-Bu groups are omitted for clarity. Symmetry codes: (i) $-x+y+1$, $-x+1$, z; (ii) $-y+1$, $x-y$, z.

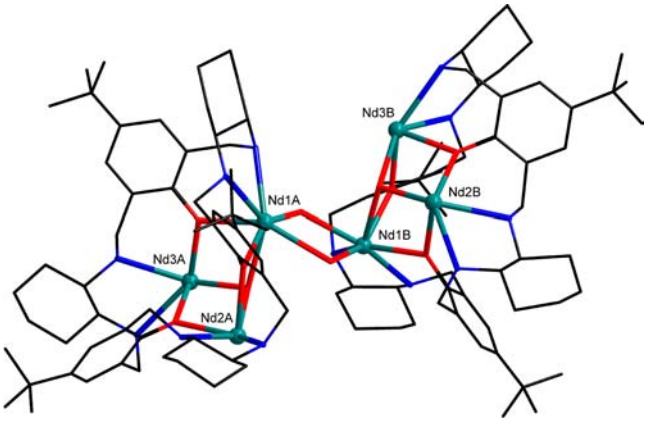

Figure 10. Model structure of $[Nd_3(\mu_3\text{-OH})]_2(\mu_2\text{-OH})_2$ cluster coordinated by two $L2^S$ macrocycyles. H atoms and axial ligands other than OH^- bridges are omitted for clarity. For the disordered region of the $L2^S$, only one position is shown.

macrocycle. Additionally two μ_2-OH bridges connect the two trinuclear macrocyclic units. In this way a $[Nd_3(\mu_3\text{-OH})]_2(\mu_2\text{-OH})_2$ cluster is coordinated by two macrocycles. Interestingly, the macrocycle adopts a highly distorted cone-shaped conformation. This conformation is somewhat similar to that of L4 (Figure 1) in its double-decker Zn(II) complex,[7] but is completely different from the more "flat" conformation observed for **12** and other Ln(III) trinuclear complexes of L1 and L2, as well as for their trinuclear transition metal complexes and free macrocycles.[4] This difference illustrates considerable flexibility of the discussed macrocycles in adjusting to particular coordination.

Magnetic Properties. Variable temperature magnetic susceptibility data for complexes **4**, **5**, **10**, and **13** were obtained in the temperature range 1.8−300 K at a magnetic field of 0.5 T. For the complex **10**, the $\chi_M T$ product is equal to 23.4 cm^3 K mol^{-1} at 300 K, which is in good agreement with the value of 23.6 cm^3 K mol^{-1} expected for three noninteracting Gd(III) ions. The the $\chi_M T$ value decreases with decreasing temperature; this decrease is initially very slight and accelerates below about 50 K with $\chi_M T$ reaching finally the value of 8.28 cm^3 K mol^{-1} at 1.8 K (Figure 11). This decrease is in accord with antiferromagnetic interaction, as for the Gd(III) ion only the ground state is populated and magnetic anisotropy is expected to be low. The antiferromagnetic interaction is also evident from the $1/\chi_M = f(T)$ plots and negative value of the Weiss constant.

The variable temperature magnetic data for **10** were simulated assuming a simplified model of a regular triangular arrangement of three identical $S = 7/2$ Gd(III) ions with isotropic exchange, which corresponds to the following spin-only Hamiltonian:

$$H = -J(S_1S_2 + S_2S_3 + S_3S_1) \quad (1)$$

The total spin state combinations and their energies were calculated using the Kambe approach[28] implemented in the MAGMUN 4.1 magnetic software package.[29] A reasonable fit ($R = [\sum(\chi_{exp} - \chi_{calc})^2/\sum(\chi_{exp})^2]^{1/2} = 0.014$) was obtained for $g = 2.00$ and $J = -0.17$ cm^{-1} (Figure 11). The magnetic behavior of **10** is very similar to that of the $Gd_3(\mu_3\text{-OH})_2$

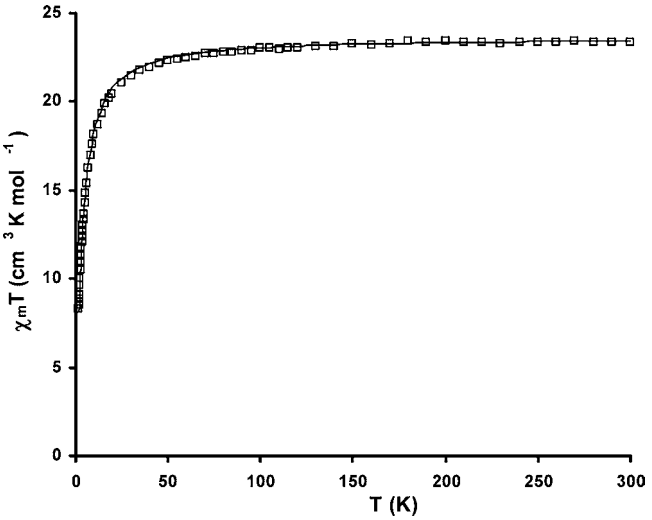

Figure 11. Temperature dependence of experimental $\chi_M T$ vs T for **10**. Solid line represents the simulated curve calculated on the basis of eq 1.

trinuclear complex[12] of *o*-vanilin ligand, where the antiferromagnetic interaction with $J = -0.19$ cm^{-1} was observed.

The RT $\chi_M T$ values for **13** (Figure 12) is equal to 40.1 cm^3 K mol^{-1}, slightly lower than the value of 42.5 cm^3 K mol^{-1} expected for the three noninteracting $^6H_{15/2}$ Dy(III) ions with $g = 4/3$ and $J = 15/2$. On cooling the $\chi_M T$ value first changes slightly in an irregular fashion, then after about 40 K increases to reach the maximum value of 41.4 cm^3 K mol^{-1} at 9 K (Figure 12). After reaching a maximum, the $\chi_M T$ values fall sharply on further cooling to 1.8 K, reaching the value of 25.0 cm^3 K mol^{-1}. The initial increase of $\chi_M T$ values may reflect ferromagnetic interactions, while the subsequent decrease of $\chi_M T$ is most likely the result of the depopulation of the sublevels of the $^6H_{15/2}$ state and magnetic anisotropy, although weak antiferromagnetic interactions may also play a role. Slightly different behavior was reported[2] for the $[Dy_3L2(\mu_3\text{-OH})_2(NO_3)_2(H_2O)_4](NO_3)_2{\cdot}6MeOH{\cdot}H_2O$ complex; where the $\chi_M T$ values initially remained constant, then slightly decreased to 37.11 cm^3 K mol^{-1} at 40 K, and then increased to reach a maximum of 42.29 cm^3 K mol^{-1} at 3 K. This difference indicates

dx.doi.org/10.1021/ic400508y | Inorg. Chem. 2013, 52, 12893−12903

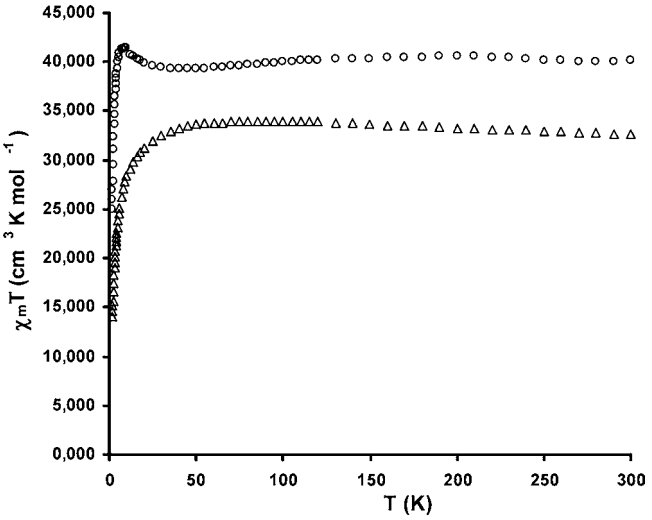

Figure 12. Temperature dependence of experimental $\chi_M T$ vs T for complex **4** (triangles) and complex **13** (circles).

the influence of minor changes in the molecular structure (the complexes differ in the set of axial ligands) on the magnetic interactions. Importantly, the susceptibility of **13** is not vanishing at low temperatures, and $\chi_M T$ values are not close to zero at 1.8 K, as it was observed for the very unusual case of nonmagnetic ground state of a system with odd number of ions with half-integer J value observed for an analogous $Ln_3(\mu_3\text{-}OH)_2$ triangle complexed with *o*-vanilin ligands.[11f] This difference and the irregular change of $\chi_M T$ with temperature, possibly reflect lowering of the C_3 symmetry in the present case, and the presence of various axial ligations for the two independent complex molecules observed in the crystal of **13**. This lowering of symmetry leads to nonequivalent interactions in the various pairs of Dy(III) ions and hence different magnetic behavior.

For complex **4** the $\chi_M T$ value of 32.6 cm^3 K mol^{-1} observed at RT is somewhat lower than the value of 35.4 cm^3 K mol^{-1} expected for three noninteracting $^7F_6$ Tb(III) ions with $g = 3/2$ and $J = 6$. The $\chi_M T$ value increases steadily as the temperature is lowered to 100 K reaching a maximum value of 34.0 cm^3 K mol^{-1}, and then after about 50 K drops to the value of 14.1 cm^3 K mol^{-1}at 1.8 K (Figure 12). Similarly as for complexes **13**, these variations may reflect both the isotropic exchange as well as of thermal depopulation of m_J sublevels and magnetic anisotropy, and the initial increase of $\chi_M T$ values may indicate weak ferromagnetic interactions.

CONCLUSIONS

The chiral macrocyclic amines $L1^{R,S}$ and $L2^{R,S}$ are suitable hosts for the encapsulation of $Ln_3(\mu_3\text{-}OH)_2$ clusters both in the solid-state and in solution, except the largest Ln(III) ions. Despite the D_3 symmetry of the free macrocycles and clusters, the X-ray crystal structures of the obtained trinuclear complexes indicate the tendency to lowering the symmetry of the system because of various axial coordination at the particular Ln(III) sites. Out of the 13 structures presented herein and 2 structures reported previously only one structure corresponds to C_3 symmetry. On the other hand an effective D_3 symmetry of the complexes is observed in solution because of dynamic exchange of axial ligands. In the case of the Nd(III) ion encapsulation of the $[Ln_3(\mu_3\text{-}OH)]_2(\mu_2\text{-}OH)_2$ cluster by two macrocycles units is additionally observed. The magnetic data indicate weak antiferromagnetic interactions in the case of the trinuclear Gd(III) complex and possible weak ferromagnetic interactions in the case of the trinuclear Dy(III) complexes.

ASSOCIATED CONTENT

Supporting Information

Figures S1−S10, Table S1, details of crystal structure solutions for hexanuclear Nd(III) complex as well as X-ray crystallographic information in CIF format. This material is available free of charge via the Internet at http://pubs.acs.org.

AUTHOR INFORMATION

Corresponding Author

*E-mail: jerzy.lisowski@chem.uni.wroc.pl. Fax: 48 71 3282348. Phone: 48 71 3757252.

Notes

The authors declare no competing financial interest.

ACKNOWLEDGMENTS

This work was supported by MNiSW Grant N N204 017135.

REFERENCES

(1) Paluch, M.; Ślepokura, K.; Lis, T.; Lisowski, J. *Inorg. Chem. Commun.* **2011**, *14*, 92−95.
(2) (a) Lin, S.-Y.; Guo, Y.-N.; Guo, Y.; Zhao, L.; Zhang, P.; Ke, H.; Tang, J. *Chem. Commun.* **2012**, *48*, 6924−6926.
(3) Paluch, M.; Lisowski, J.; Lis, T. *Dalton Trans.* **2006**, 381−388.
(4) (a) Kobyłka, M. J.; Janczak, J.; Lis, T.; Kowalik-Jankowska, T.; Kłak, J.; Pietruszka, M.; Lisowski, J. *Dalton Trans.* **2012**, *41*, 1503−1511. (b) Gao, J.; Zingaro, R. A.; Reibenspies, J. H.; Martell, A. E. *Org. Lett.* **2004**, *6*, 2453. (c) Korupoju, S. R.; Mangayarkarasi, N.; Zacharias, P. S.; Mizuthani, J.; Nishihara, H. *Inorg. Chem.* **2002**, *41*, 4099.
(5) (a) Gregoliński, J.; Starynowicz, P.; Hua, K. T.; Lunkley, J. L.; Muller, G.; Lisowski, J. *J. Am. Chem. Soc.* **2008**, *130*, 17761−17773. (b) Gregoliński, J.; Lis, T.; Cyganik, M.; Lisowski, J. *Inorg. Chem.* **2008**, *47*, 11527−11534. (c) Gregoliński, J.; Lisowski, J. *Angew. Chem., Int. Ed.* **2006**, *45*, 6122−6126.
(6) González-Alvarez, A.; Alfonso, I.; Cano, J.; Díaz, P.; Gotor, V.; Gotor-Fernández, V.; García-España, E.; Garcia-Granda, S.; Jiménez, H. R.; Lloret, G. *Angew. Chem., Int. Ed.* **2009**, *48*, 6055−6058.
(7) Sarnicka, A.; Starynowicz, P.; Lisowski, J. *Chem. Commun.* **2012**, *48*, 2237−2239.
(8) (a) Train, C.; Gruselle, M.; Verdaguer, M. *Chem. Soc. Rev.* **2011**, *40*, 3297−3312. (b) Train, C.; Gheorghe, R.; Krstic, V.; Chamoreau, L.-M.; Ovanesyan, M. S.; Rikken, G. L. J. A.; Gruselle, M.; Verdaguer, M. *Nat. Mater.* **2008**, *7*, 729−734.
(9) (a) De Leon-Rodriguez, L. M.; Lubag, A. J. M.; Malloy, C. R.; Martinez, G. V.; Gillies, R. J.; Sherry, A. D. *Acc. Chem. Res.* **2009**, *42*, 948−957. (b) Bottrill, M.; Kwok, L.; Long, N. J. *Chem. Soc. Rev.* **2006**, *35*, 557−571. (c) Jacques, V.; Desreux, J. F. *Top. Curr. Chem.* **2002**, *221*, 123−164. (d) Caravan, P.; Ellison, J. J.; McMurry, T. J.; Lauffer, R. B. *Chem. Rev.* **1999**, *99*, 2293−2359. (e) Yam, V. W.-W.; Lo, K. K.-W. *Coord. Chem. Rev.* **1999**, *184*, 157−240.
(10) Caravan, P. *Chem. Soc. Rev.* **2006**, *35*, 512−523.
(11) (a) Lin, S.-Y.; Zhao, L.; Guo, Y.-N.; Zhang, P.; Guo, Y.; Tang, J. *Inorg. Chem.* **2012**, *51*, 10522−10528. (b) Hewitt, I. J.; Tang, J.; Madhu, N. T.; Anson, C. E.; Lan, Y.; Luzon, J.; Etienne, M.; Sessoli, R.; Powell, A. K. *Angew. Chem., Int. Ed.* **2010**, *49*, 6352−6356. (c) Sessoli, R.; Powell, A. K. *Coord. Chem. Rev.* **2009**, *253*, 2328−2341. (d) Andrews, P. C.; Deacon, G. B.; Frank, R.; Fraser, B. H.; Junk, P. C.; MacLellan, J. G.; Massi, M.; Moubaraki, B.; Murray, K. S.; Silberstein, M. *Eur. J. Inorg. Chem.* **2009**, 744−751. (e) Chibotaru, L. F.; Ungur, L.; Soncini, A. *Angew. Chem., Int. Ed.* **2008**, *47*, 4126−4129. (f) Tang, J.; Hewitt, I.; Madhu, N. T.; Chastanet, G.; Wernsdorfer, W.; Anson, C. E.; Benelli, C.; Sessoli, R.; Powell, A. K. *Angew. Chem., Int. Ed.* **2006**, *45*, 1729−1733.

(12) Costes, J.-P.; Dahan, F.; Nicodème, F. *Inorg. Chem.* **2001**, *40*, 5285−5287.
(13) (a) Vallejo, J.; Cano, J.; Castro, I.; Julve, M.; Lloret, F.; Fabelo, O.; Cañadillas-Delgado, L.; Pardo, E. *Chem. Commun.* **2012**, *48*, 7726−7728. (b) Langley, S. K.; Moubaraki, B.; Murray, K. S. *Inorg. Chem.* **2012**, *51*, 3947−3949. (c) Anwar, M. U.; Tandon, S. S.; Dawe, L. N.; Habib, F.; Murugesu, M.; Thompson, L. K. *Inorg. Chem.* **2012**, *51*, 1028−1034. (d) Guo, Y.-N.; Xu, G.-F.; Wernsdorfer, W.; Ungur, L.; Guo, Y.; Tang, J.; Zhang, H.-J.; Chibotaru, L. F.; Powell, A. K. *J. Am. Chem. Soc.* **2011**, *133*, 11948−11951. (e) Hewitt, I. J.; Lan, Y.; Anson, C. E.; Luzon, J.; Sessoli, R.; Powell, A. K. *Chem. Commun.* **2009**, 6765−6767. (f) Gamer, M. T.; Lan, Y.; Roesky, P. W.; Powell, A. K.; Clérac, R. *Inorg. Chem.* **2008**, *47*, 6581−6583.
(14) (a) Peng, J.-B.; Zhang, Q.-C.; Kong, X.-J.; Zheng, Y.-Z.; Ren, Y.-P.; Long, L.-S.; Huang, R.-B.; Zheng, L.-S.; Zheng, Z. *J. Am. Chem. Soc.* **2012**, *134*, 3314−3317. (b) Novitchi, G.; Wernsdorfer, W.; Chibotaru, L. F.; Costes, J.-P.; Anson, C. E.; Powell, A. K. *Angew. Chem., Int. Ed.* **2009**, *48*, 1614−1619. (c) Aronica, C.; Pilet, G.; Chastanet, G.; Wernsdorfer, W.; Jacquot, J.-F.; Luneau, D. *Angew. Chem., Int. Ed.* **2006**, *45*, 4659−4662. (d) Osa, S.; Kido, T.; Matsumoto, N.; Re, N.; Pochaba, A.; Mroziński, J. *J. Am. Chem. Soc.* **2004**, *126*, 420−421.
(15) (a) Krężel, A.; Lisowski, J. *J. Inorg. Biochem.* **2012**, *107*, 1−5. (b) Camargo, M. A.; Neves, A.; Bortoluzzi, A. J.; Szpoganicz, B.; Fischer, F. L.; Terenzi, H.; Serrra, O. A.; Santos, V. G.; Vaz, B. G.; Eberlin, M. N. *Inorg. Chem.* **2010**, *49*, 6013−6025. (c) Chang, C. A.; Wu, B. H.; Hsiao, C.-H. *Eur. J. Inorg. Chem.* **2009**, 1339−1346. (d) Liu, C.; Wang, L. *Dalton Trans.* **2009**, 227−239. (e) Sanchez-Lombardo, I.; Yatsimirsky, A. K. *Inorg. Chem.* **2008**, *47*, 2514−2525. (f) Farquhar, E. R.; Richard, J. P.; Morrow, J. R. *Inorg. Chem.* **2007**, *46*, 7169−7177. (g) Aguilar-Perez, F.; Gomez-Tagle, P.; Collorado-Fregoso, E.; Yatsimirsky, A. K. *Inorg. Chem.* **2006**, *45*, 9502−9517. (h) Chang, C. A.; Wu, B. H.; Kuan, B. Y. *Inorg. Chem.* **2005**, *44*, 6646−6654. (i) Jurek, P. E.; Jurek, A. M.; Martell, A. E. *Inorg. Chem.* **2000**, *39*, 1016−1020. (j) Hurst, P.; Takasaki, B. K.; Chin, J. *J. Am. Chem. Soc.* **1996**, *18*, 9982−9983. (k) Liu, C.; Wang, M.; Zhang, T.; Sun, H. *Coord. Chem. Rev.* **2004**, *248*, 147−168.
(16) (a) Yang, X.; Hahn, B. P.; Jones, R. A.; Wong, W.-K.; Stevenson, K. J. *Inorg. Chem.* **2007**, *46*, 7050−7054. (b) Wang, R.; Song, D.; Wang, S. *Chem. Commun.* **2002**, 368−369. (c) Zheng, Z. *Chem. Commun.* **2001**, 2521−2529.
(17) (a) Arnold, P. L.; Potter, N. A.; Carmichael, C. D.; Slawin, A. M. Z.; Roussel, P.; Love, J. B. *Chem. Commun.* **2010**, *46*, 1833−1835. (b) Thielemann, D.; Fernandez, I.; Roesky, P. W. *Dalton Trans.* **2010**, *39*, 6661−6666. (c) Stomeo, F.; Lincheneau, C.; Leonard, J. P.; O'Brien, J. E.; Peacock, R. D.; McCoy, C. P.; Gunnlaugsson, T. *J. Am. Chem. Soc.* **2009**, *131*, 9636−9637. (d) Kong, X.-J.; Wu, Y.; Long, L.-S.; Zheng, L.-S.; Zheng, Z. *J. Am. Chem. Soc.* **2009**, *131*, 6918−6919. (e) Albrecht, M.; Schimid, S.; Dehn, S.; Wickleder, C.; Zhang, S.; Bassett, A. P.; Pikramenou, Z.; Fröhlich, R. *New J. Chem.* **2007**, *31*, 1755−1762. (f) Jeong, K. S.; Kim, Y. S.; Kim, Y. J.; Lee, E.; Yoon, J. H.; Park, W. H.; Park, Y. W.; Jeon, S.-J.; Kim, Z. H.; Kim, J.; Jeong, N. *Angew. Chem., Int. Ed.* **2006**, *45*, 8134−8138. (g) Thompson, M. K.; Lough, A. J.; White, A. J. P.; Williams, D. J.; Kahwa, I. A. *Inorg. Chem.* **2003**, *42*, 4828−4841.
(18) (a) Bozoklu, G.; Gateau, C.; Imbert, D.; Pécaut, J.; Robeyns, K.; Filinchuk, Y.; Memon, F.; Muller, G.; Mazzanti, M. *J. Am. Chem. Soc.* **2012**, *134*, 8372−8375. (b) Bozoklu, G.; Marchal, C.; Gateau, C.; Pécaut, J.; Imbert, D.; Mazzanti, M. *Chem.—Eur. J.* **2010**, *16*, 6159−6163. (c) Murray, B. S.; Parker, D.; dos Santos, C. M. G.; Peacock, R. D. *Eur. J. Inorg. Chem.* **2010**, 2663−2672. (d) Lama, M.; Mamula, O.; Kottas, G. S.; De Cola, L.; Stoeckli-Evans, H.; Shova, S. *Inorg. Chem.* **2008**, *47*, 8000−8015. (e) Lama, M.; Mamula, O.; Kottas, G. S.; Rizzo, F.; De Cola, L.; Nakamura, A.; Kuroda, R.; Stoeckli-Evans, H. *Chem.—Eur. J.* **2007**, *13*, 7358−7373. (f) Mamula, O.; Lama, M.; Stoeckli-Evans, H.; Shova, S. *Angew. Chem., Int. Ed.* **2006**, *45*, 4940−4944. (g) Mamula, O.; Lama, M.; Telfer, S. G.; Nakamura, A.; Kuroda, R.; Stoeckli-Evans, H.; Scopelitti, R. *Angew. Chem., Int. Ed.* **2005**, *44*, 2527−2531. (h) Natrajan, L.; Pécaut, J.; Mazzanti, M.; LeBrun, C. *Inorg. Chem.* **2005**, *44*, 4756−4765.
(19) Lisowski, J. *Inorg. Chem.* **2011**, *50*, 5567−5576.
(20) (a) Kong, X.-J.; Wu, Y.; Long, L.-S.; Zheng, L.-S.; Zheng, Z. *J. Am. Chem. Soc.* **2009**, *131*, 6918−6919. (b) Kong, X.-J.; Long, L.-S.; Zheng, L.-S.; Wang, R.; Zheg, Z. *Inorg. Chem.* **2009**, *48*, 3268−3273. (c) Zhang, M.-B.; Zhang, J.; Zheng, S.-T.; Yang, G.-Y. *Angew. Chem., Int. Ed.* **2005**, *44*, 1385−1388. (d) Fang, X.; Andreson, T. M.; Benelli, C.; Hill, C. L. *Chem.—Eur. J.* **2005**, *11*, 712−718. (e) Wang, R.; Selby, H. D.; Liu, H.; Carducci, M. D.; Jin, T.; Zheng, Z.; Anthis, J. W.; Staples, R. J. *Inorg. Chem.* **2002**, *41*, 278−286.
(21) (a) Chen, L.-F.; Zhang, J.; Ren, G.-Q.; Li, Z.-J.; Qin, Y.-Y.; Yin, P.-X.; Cheng, J.-K.; Yao, Y.-G. *CrystEngComm* **2008**, *10*, 1088−1092. (b) Zhang, L.-Z.; Gu, W.; Li, B.; Liu, X.; Liao, D.-Z. *Inorg. Chem.* **2007**, *46*, 622−624. (c) Hu, M.; Wang, Q.-L.; Xu, G.-F.; Zhao, B.; Deng, G.-R.; Zhang, Y.-H.; Yang, G.-M. *Inorg. Chem. Commun.* **2007**, *10*, 1177−1180. (d) Zhang, M.-B.; Zhang, J.; Zheng, S.-T.; Yang, G.-Y. *Angew. Chem., Int. Ed.* **2005**, *44*, 1385−1388. (e) Zheng, X.-J.; Jin, L.-P.; Gao, S. *Inorg. Chem.* **2004**, *43*, 1600−1602.
(22) Korupoju, S. R.; Zacharias, P. S. *Chem. Commun.* **1998**, 1267.
(23) Bain, G. A.; Berry, J. F. *J. Chem. Educ.* **2008**, *85*, 532-536.
(24) *Crysalis CCD and Crysalis RED in Xcalibur PX or Kuma KM4CCD Software*; Oxford Diffraction Ltd.: Abingdon, England, 2009.
(25) Sheldrick, G. M. *Acta Crystallogr., Sect. A* **2008**, *64*, 112−122.
(26) Brandenburg, K. *DIAMOND*, Version 3.0; Crystal Impact GbR: Bonn, Germany, 2005.
(27) Kobyłka, M. J.; Ślepokura, K.; Lisowski, J., unpublished results.
(28) Kambe, K. *J. Phys. Soc. Jpn.* **1950**, *5*, 48−51.
(29) Xu, Z.; He, K.; Thompson, L. K.; Waldman, O. *MAGMUN 4.1*; Memorial University of Newfoundland: St. John's, Newfoundland and Labrador, Canada, 2002.